J Mol Hist (2014) 45:91–102
DOI 10.1007/s10735-013-9531-6

ORIGINAL PAPER

Histomorphological evaluation of maternal and neonatal distal airspaces after maternal intake of nanoparticulate titanium dioxide: an experimental study in Wistar rats

Yasser M. Elbastawisy · Shaima M. Almasry

Received: 19 June 2013 / Accepted: 6 August 2013 / Published online: 10 August 2013

Abstract This study was performed to determine the histomorphological alterations occurring in maternal and neonatal pulmonary distal airspaces of Wistar rats after maternal administration of titanium dioxide nanoparticles (TiO_2 NPs). Thirty adult pregnant rats (150–250 g) and their offspring were used in this study. Pregnant rats were randomly divided into control (n = 15) and TiO_2 NP-treated (n = 15) groups. A suspension of TiO_2 NPs in phosphate-buffered saline was given orally to the treated group (0.1 ml/10 g body weight once daily) from days 6 to 12 of gestation. At term, maternal and neonatal lungs were collected and processed for energy-dispersive X-ray (EDX) and histological analysis. The mean linear intercept (MLI) and airspace wall thickness were measured by a stereological procedure with image analysis to assess alveolarization. EDX analysis demonstrated the presence of TiO_2 in maternal and neonatal lungs. The lungs of TiO_2 NP-treated mothers revealed evidence of pneumocytic apoptosis, abnormal lamellar inclusions, and macrophage and inflammatory cell infiltrates. Significant thinning of alveolar septa was detected in the treated rats ($p < 0.001$), but the MLI was constant in both groups ($p = 0.207$). Neonatal lungs from treated mothers revealed deficient septation, thickened mesenchyme between the saccules, pneumocytic apoptosis, atypical lamellar inclusions, and macrophage infiltration. The thickness of the primary septa was significantly increased ($p = 0.001$) with no significant change in MLI ($p = 0.579$) compared with the control group. In conclusion, TiO_2 NPs were detected in maternal and neonatal lungs after oral intake by pregnant rats. The pulmonary response manifested as inflammatory lesions and delayed saccular development in neonates.

Keywords Pulmonary distal airspaces · Nanoparticulate · Titanium oxide · Rats

Introduction

Titanium dioxide (TiO_2) is a fine, white, crystalline, odorless powder that is considered to exhibit relatively low toxicity (Zhang et al. 2000). According to the National Nanotechnology Initiative of America, nanosized TiO_2 particles are among those most widely manufactured on a global scale (Liang et al. 2009). Sources of TiO_2 nanoparticles (NPs) relevant for oral exposure comprise mainly cosmetics (sunscreen, lipsticks, skin creams, toothpaste) and food (packaging, storage life sensors, food additives, juice clarifiers) (Weir et al. 2012).

The health and safety aspects of NPs are still in the formative phase, and greater effort is needed to understand how NPs interact with the human body (Yokel and Macphail 2011). In this regard, nanotoxicology and nanorisk have been attracting increased attention from toxicologists and regulatory scientists (Oberdörster et al. 2005), particularly in relation to the unique properties of NPs that may render them potentially more dangerous than their fine-sized counterparts and may cause unexpected adverse health effects following human exposure (Li and Nel

Y. M. Elbastawisy · S. M. Almasry
Department of Anatomy, Taibah University, Al-Madinah Al-Munawarah, Saudi Arabia

Y. M. Elbastawisy · S. M. Almasry (✉)
Department of Anatomy and Embryology, Al-Mansoura University, Al-Mansoura, Egypt
e-mail: shaima.masry@yahoo.com

2011). Such manufacturing and consumer use can produce multiple and different sources of release of these materials into the environment, ecosystem, water and food supplies, and other routes of non-voluntary exposure into the human body (Jones and Grainger 2009). It is important, however, to distinguish between crystal forms of TiO_2 (i.e., rutile versus anatase) when considering their toxicity. One study, in particular, demonstrated that anatase TiO_2 NPs resulted in lactate dehydrogenase leakage and widespread necrosis, whereas rutile NPs resulted in higher levels of reactive oxygen species and consequently apoptosis (Braydich-Stolle et al. 2009). This study also demonstrated that although the literature supports a higher level of toxicity for anatase NPs (Wang et al. 2007; Sugibayashi et al. 2008), there is some evidence that rutile NPs, often assumed to induce less of an effect, can produce signs of toxicity.

Fetuses are known to be more sensitive to environmental toxins than adults (Koren et al. 1998), and it has been suggested that many chemical toxins in air, water, and food can induce pregnancy complications (Wigle et al. 2008). For instance, some studies have shown transplacental transport of nanomaterials in pregnant animals and nanomaterial-induced neurotoxicity in their offspring (Tian et al. 2009; Saunders 2009; Chu et al. 2010; Hougaard et al. 2010).

Considering the relevance of the respiratory system as a route for TiO_2 NPs exposure in humans, a number of previous studies (Chen et al. 2006; Fujita et al. 2009; Li et al. 2013) were conducted to study the effects of inhalation of these particles on the respiratory system. However, to our knowledge, this is the first study that investigates the histomorphological alterations in maternal and neonatal pulmonary distal airspaces of Wistar rats after oral administration of TiO_2 NPs by mothers.

Materials and methods

Experimental animals

Fifteen adult male and 30 adult female albino Wistar Han rats (150–250 g) were obtained from the Animal Breeding Unit of Assiut University (Egypt) and kept under constant conditions, a 12:12 light/dark cycle, and a room temperature of 28 °C. They were allowed access to a standard rat chow diet and water ad libitum, and food intake and body weight were recorded daily throughout the experimental period. Prior to dosing, animals were acclimated to the environment for 7 days. National Institutes of Health (NIH) guidelines for the care and use of laboratory animals (NIH Publication 85–23 Rev. 1985) were observed.

Mating procedure

Males were individually housed. Two females were placed into a cage with one male overnight (12 h). The following morning, mating was confirmed if a vaginal plug was observed, which served as day 0 of the pregnancy (GD0).

Pregnant rats were divided randomly into two main groups: age-matched controls (n = 15) and TiO_2 NP-treated rats (n = 15). The control rats received a balanced standard diet together with the vehicle, phosphate-buffered saline (PBS).

Nanoparticles

Titanium dioxide nanopowder was obtained from Sigma-Aldrich Co. (St. Louis, MO, USA; product 718467, CAS number 13463-67-7). According to the product sheet, the nanopowder was approximately 21 nm (TEM), specific surface area: 35–65 m^2/g (BET), density: 4.26 g/ml at 25 °C, molecular weight: 79.87 and purity: 99.5 %. Nano-TiO_2 (5 g/kg body weight) was suspended into PBS, and then the suspension was ultrasonicated before it was used to treat animals to avoid aggregation and provide an optimum size distribution for dispersed particle agglomerates.

Treatment of animals

The methodology adopted was that of Zhang et al. (2010). Before treatment, animals were fasted overnight. TiO_2 nanoparticles, in a stable suspending state, were diluted to 20 mg/ml. Subsequently, the TiO_2 suspension was administered to the treated group via oral gavage in doses of 0.1 ml/10 g body weight once daily for 7 consecutive days (GD6-12). The control rats were treated with PBS daily for the same period. Food and water were provided 2 h later.

Prenatal evaluation

Maternal behavioral changes, body weight, and quantity of food and water consumption were evaluated daily from GD0 to GD21. The presence of vaginal bloodstains demonstrated the process of abortion or fetal expulsion.

Tissue sampling and processing

On GD21, after previous anesthesia with carbon monoxide, cesarean sections were performed on all pregnant females. Subsequently, the females were sacrificed, and the lungs were separated and weighed. The rat pups were extracted, counted, and examined for external variation. Finally, the rat pups were carefully dissected, and all lungs were harvested. Pressure control and lung fixation was performed as adopted by Vlahovic et al. (1999). Simply, 2 % glutaraldehyde in

0.085 sodium cacodylate buffer (pH 7.4) was instilled through syringes, which were inserted into the airways of collapsed lobes or lung segments. The fixative was instilled quickly to obtain rapid filling of the lung tissue, but over-distension was avoided through careful observation. The alveolar tissue became rigid within seconds and maintained full inflation even though there was a cut surface on the surgically obtained lung lobes.

Pulmonary ultrastructure analysis

After application of the fixative, the tissue remained in the fixative for 24 h, and the specimens for transmission electron microscope (TEM) were postfixed in 0.085 sodium cacodylate buffered 2 % osmium tetroxide in the same buffer at 4 °C, dehydrated using a series of ethanol concentrations, and embedded in epoxy resin.

Semi-thin sections (0.5–1 μm) were cut using a knife with a liquid-filled boat, removed from the boat with a clean wire loop, and transferred to a drop of water on a clean glass slide. The slides were then placed on a low temperature hot plate. The sections were then stained with toluidine blue and evaluated by a histopathologist unaware of the treatments using light microscopy (U-III Multi-point Sensor System; Nikon, Tokyo, Japan).

Ultrathin sections (50–70 nm thick) were stained with uranyl acetate and lead citrate and examined and photographed using a JEOL JEM 1200 EXII Electron Microscope (Jeol Ltd.) Research Laboratory, Assiut University, Egypt (Glauert and Lewis 1998).

Energy-dispersive X-ray (EDX) analysis

Analysis of the TiO_2 in the tissue was conducted using an EDX unit attached to a scanning electron microscope (SEM) using glutaraldehyde-fixed carbon dried tissue samples. EDX uses the X-ray spectrum emitted by a solid sample bombarded with a focused beam of electrons to obtain a localized chemical analysis (Agarwal 1991; Scott and Love 1994).

Morphometric lung analysis

Measurement of the interalveolar wall distance was assessed in the adult and neonatal lungs by measuring the mean linear intercept (MLI) (described later in detail). Additionally, the airspace wall thickness, as an indication of the thickness (width) of the septa, was measured directly used an Image Analyzer (Leica Q Win standard, digital camera CH-9435 DFC 290, Germany). The measuring tool was applied to the middle as well as to the marginal parts of the septa to uniformly compute the mean width of whole septa. Measurements were conducted for each lung on five fields (at 200× magnification; frame area = 786,432.0 μ^2) and performed by an investigator who was unaware of the identity of the samples.

Method of intercept or chord length estimation

Mean linear intercept is the mean length of straight-line segments (chords) on random test lines crossing the air-space between two sequential intersections of the alveolar surface with the test line. The chord lines often cross from one alveolus through an alveolar duct to an opposite alveolus, indicating that the MLI characterizes the entire acinar airspace complex (alveoli + ducts) and not just alveoli (Fig. 1) (Knudsen et al. 2010).

Results

Particle characterization

Titanium dioxide nanopowder is hydrophilic, and TEM has shown that it is present mostly as agglomerations of smaller particles that are 114–122 nm in diameter, which indicates that the majority of TiO_2 NPs were clustered and aggregated in solution.

Prenatal evaluation of maternal and fetal parameters

Table 1 shows the effects of TiO_2 NPs ingestion on pregnant rats during the prenatal period. No mortality or treatment-related evident signs of maternal toxicity, stress or abnormal behavioral changes were observed. None of the pregnant rats exhibited vaginal bleeding or expulsions of products of conception. The food and water intakes, maternal weight gain, and lung weights of the treated rats were not statistically ($p > 0.05$) different from that of the control group.

Titanium dioxide content analysis

In the adult and fetal experimental groups, the contents of titanium in lung, brain, liver, and kidney tissues of female Wistar rats were measured 9 days after the last dose of TiO_2 NPs. The highest amount of titanium was found in the maternal and neonatal lungs (0.82 ± 0.15 and 0.4 ± 0.53 ng/g, respectively) (Fig. 2a, b), which was confirmed by further histological examination of the lungs.

Histological examination of maternal lung tissue

Histological examination of the semi-thin sections of the adult control lung samples revealed normal architecture of

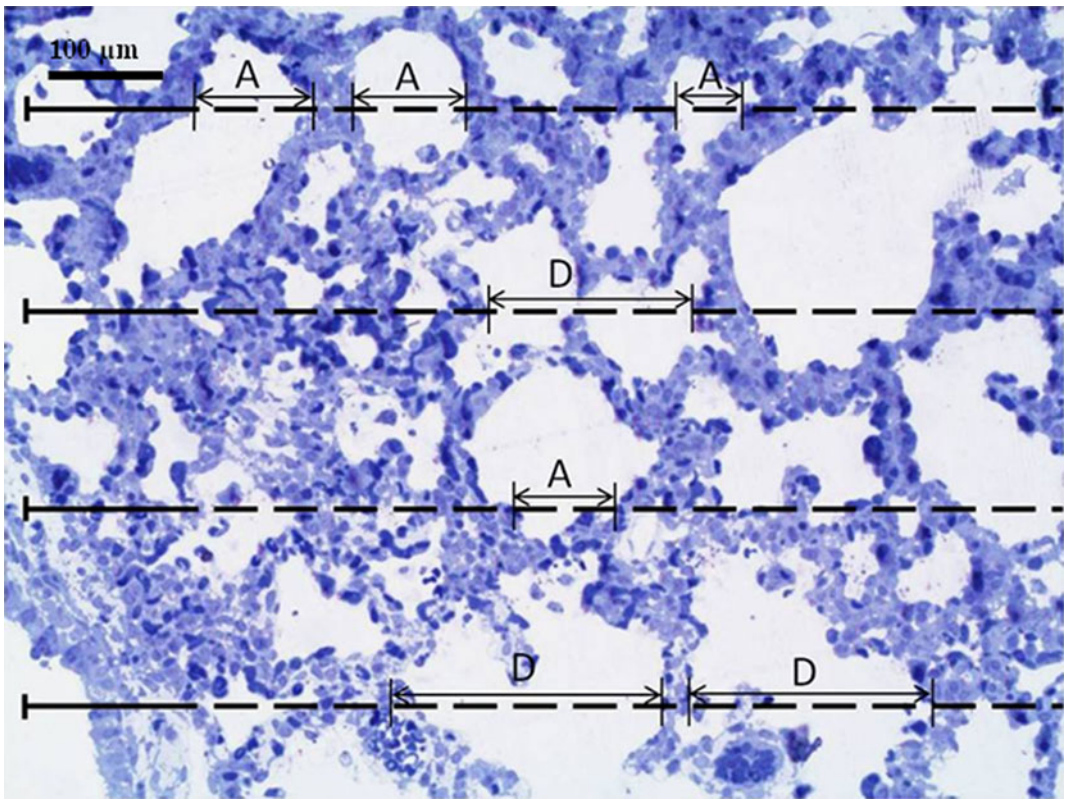

Fig. 1 A photomicrograph of the control neonatal lung shows the method of direct estimation of MLI length based on intercept distribution. Random linear intercepts were measured on microscopic images: test line segments are localized at *left* (of known length), followed by a *dashed line* toward the *right*. Each time the test line intersects the alveolar wall, the distance (intercept length) to the next wall is measured. Boundaries of measurements within alveolar airspace (*A*) or alveolar and ductal airspace together (*D*) are marked by *arrows* (toluidine blue ×200). This figure is modified from Knudsen et al. (2010)

Table 1 Maternal effects of TiO_2 NP ingestion (5 g/kg body weight) by pregnant rats before and during organogenesis (GD1–GD20)

Parameter	Control adults ($n = 15$)	Treated adults ($n = 15$)	p value
No. of pups	13	12	
No. of dead pups	2	3	
No. of fetal expulsions	0	0	
Food consumption [g/(kg day)]	77.8 ± 1	79.3 ± 1	0.37
Water utilization [ml/(kg day)]	68.8 ± 0.8	67.8 ± 1.2	0.51
Maternal weight (GD0, g)	189.3 ± 8.5	191.9 ± 7.3	0.82
Maternal weight (GD20, g)	225 ± 8.7	226.9 ± 6.7	0.88
Maternal weight gain (g)	35.9 ± 1.3	35.1 ± 2.1	0.73
Lung weight (g)	1.41 ± 0.01	1.42 ± 0.01	0.80

Data are given as the mean ± SE; data were analyzed by independent *t* test. Significant difference among groups was observed; * $p > 0.05$

the alveolar sacs and alveoli. The wall of the alveoli was lined by a single layer of pneumocytes that were composed of type I and type II pneumocytes. Pneumocytes were separated by thin septa and surrounded by a plexus of capillaries constituting the blood-air barrier (Fig. 3a, a′). TEM examination revealed type I and type II pneumocytes having euchromatic nuclei and multiple mitochondria. The latter cells contained many lamellar inclusions with identical pulmonary surfactant and possessed microvilli protruding into the airway spaces (Fig. 4a, a′).

In contrast, semi-thin sections of the lungs exposed to TiO_2 NPs exhibited various histological and morphological changes, including a focal decrease in the alveolar wall thickness, widening of the pulmonary interstitium, and inflammatory cell infiltrates. Additionally, there was an interstitial deposition of multiple dense deposits (Fig. 3b, b′). TEM showed type II pneumocytes with heterochromatic nuclei, atypical lamellar bodies, vacuolated cytoplasm, and short microvilli. There were numerous particle-laden interstitial macrophages with heterochromatic nuclei

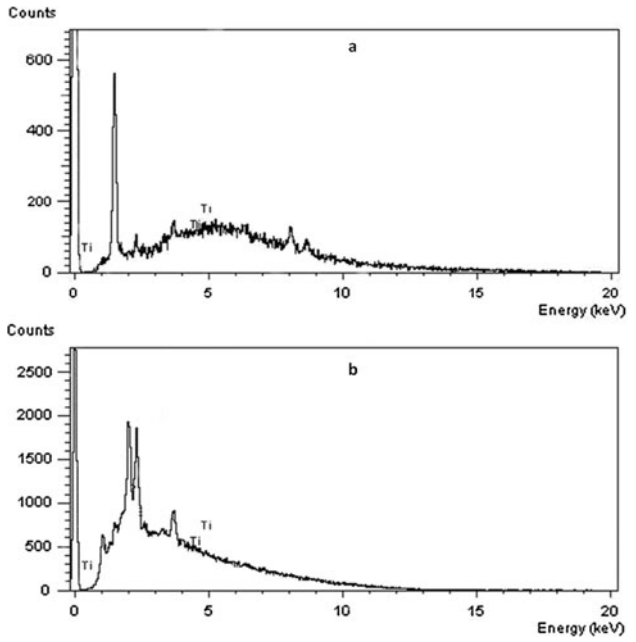

Fig. 2 The EDX spectrum of adult (**a**) and neonatal (**b**) lungs after ingestion of a single dose of 20 nm TiO_2 nanoparticles

and apical pseudopodia. Multiple black precipitates were observed in the tissues, and the observed histological changes were noticed to be more obvious in these areas of the black precipitates (Fig. 4b, b′).

Histological examination of neonatal lung tissue

Histological examination of the semi-thin sections of the neonatal lungs from unexposed mothers showed many saccules constituting immature alveoli and many intervening airways representing immature alveolar ducts. Immature alveoli were separated by many buds constituting the primary septa that varied in their thickness (Fig. 5a, a′). TEM examination revealed interalveolar septa with type I and type II pneumocytes surrounded by a circle of capillaries. Type I pneumocytes exhibited common basement membranes with an endothelium of the blood capillaries (Fig. 6a).

In comparison, semi-thin sections of neonatal lungs from TiO_2 NP-treated mothers revealed poorly developed respiratory saccules with interrupted primary septa and focal thickening of the intervening mesenchyme. There were numerous alveolar macrophages scattered in the alveolar wall and free within the airspaces, and their cytoplasms were burdened with dense-stained particles. There were many interstitial cells, and the interstitial spaces contained multiple dense deposits (Fig. 5b, b′). TEM examination showed a thick saccular wall containing interstitial cells, some of which appeared apoptotic with shrunken nuclei and lipid droplets. Additionally, there were numerous type II pneumocytes having dark cytoplasm, shrunken eccentric nuclei, many apparent atypical lamellar bodies, few short microvilli, and variable-sized vesicles containing electron dense particles. There were many interstitial macrophages with irregular nuclei and numerous lysosomes (Fig. 6b, c).

Morphometric analysis

The measurements obtained from the pulmonary alveoli of adult rats are presented in Fig. 7a. The mean linear intercept was slightly lower in the TiO_2 NP-treated rats compared with the control group (mean, 108.8 ± 6.9 vs. 101.6 ± 5.6 μm in the control and treated groups, respectively) with no significant difference between the groups ($p = 0.207$). However, there was a significant reduction in the thickness of the alveolar walls in the treated rats (mean, 76.9 ± 2.2 vs. 25.1 ± 0.9 μm; $p < 0.001$ in the control and treated groups, respectively) compared with the control group.

The measurements obtained from the pulmonary alveoli of neonatal pups are presented in Fig. 7b. The mean linear intercept was nearly similar in both groups (mean, 95.7 ± 5.9 vs. 94.9 ± 6.9 μm in the control and treated groups, respectively) with no significant difference ($p = 0.579$) between groups. However, there was a significant increase in the thickness of the alveolar walls after administration of TiO_2 NPs (mean, 85.5 ± 1.9 vs. 105.4 ± 3.8 μm; $p = 0.001$ in the control and treated groups, respectively) compared with the control group.

Discussion

Large human populations in the world continue to be exposed to pollutants. TiO_2 is one type of widely used nanoparticle that has proven hazardous to humans. Through this study, we established novel data about the deposition of TiO_2 NPs in maternal and neonatal lungs after 9 days from its maternal administration by an oral route. The presence of these nanoparticles in lung tissue was accompanied by histomorphometric alterations and neonatal alveolar maldevelopment.

In the present study, we used EDX in conjunction with SEM to analyze the energy levels of the dried lung tissue samples from rat mothers administered TiO_2 NPs and established the presence of TiO_2 in the tissues. Additionally, TEM examination displayed considerable black aggregates inside different pulmonary components as follows: the alveolar epithelium, alveolar spaces and in the interstitium, which further confirms that this substance accessed the pulmonary interstitium. These data prove the transition of TiO_2 NPs from the systemic circulation after intake by mouth to pulmonary tissue. Permeation through

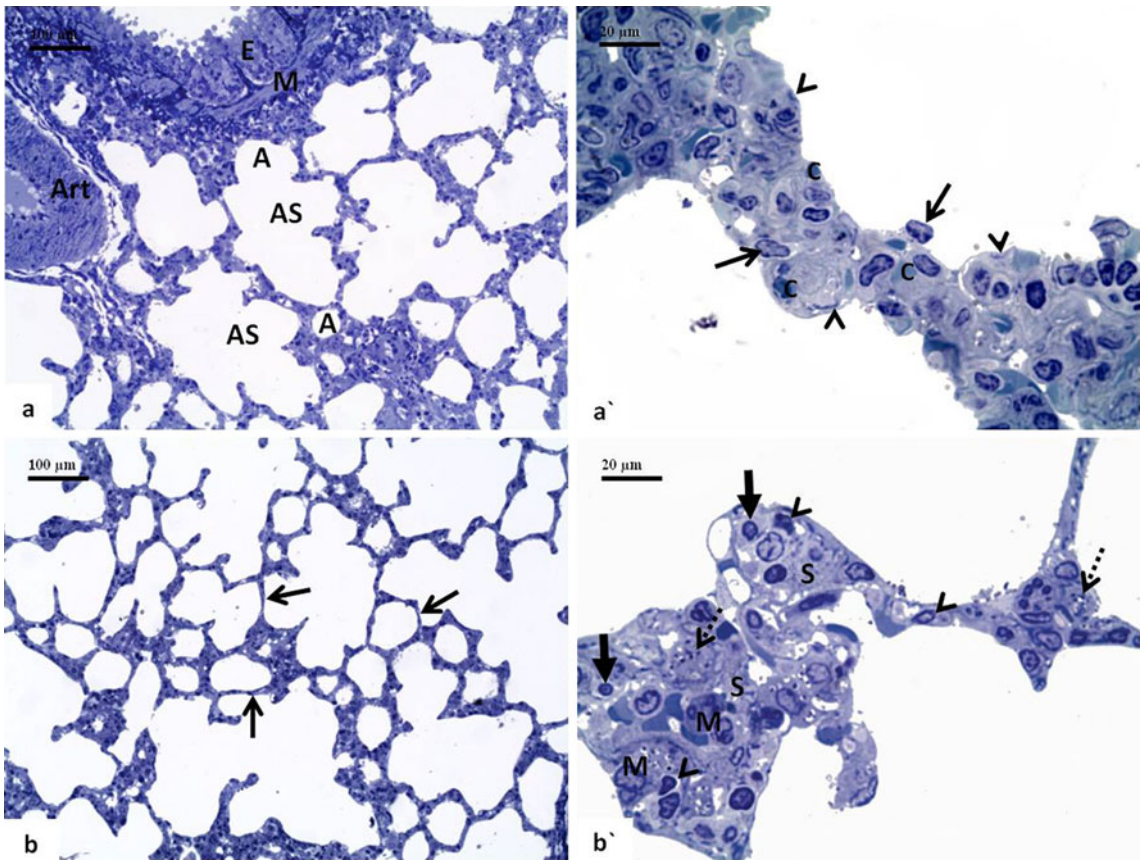

Fig. 3 Micrographs **a**, **a′** show the light microscopic appearance of the control adult lung. Alveolar sacs (*AS*) are seen open into numerous alveoli (*A*). A terminal bronchiole is seen lined with ciliated columnar epithelium (*E*) with observable smooth muscle layer (*M*). A distinct pulmonary artery branch is found next to the bronchiole (*Art*). The *right panel* shows that the wall of alveoli is lined by type I pneumocytes (*arrowheads*) with flattened nuclei and type II pneumocytes (*arrows*) with large plump nuclei. A number of capillaries (*c*) form plexus around the alveoli. Micrographs **b**, **b′** show the light microscopic appearance of TiO_2 NP-treated adult lung with apparent thinning of airway septa in many areas (*thin arrows*). The *right panel* shows apparent widening of pulmonary interstitium (*S*) and infiltration of lymphocytes (*thick arrows*) and interstitial macrophages (*M*). Multiple dense deposits are present in the interstitial spaces of the alveolar walls (*dashed arrows*), and many apoptotic cells are observed (*arrowheads*) [**a**, **b** toluidine blue ×200—**a′**, **b′** toluidine blue ×1,000]

the gastrointestinal barriers has been shown previously for micro- and nano-particles. These barriers consist of cellular (epithelium) and acellular parts (dead cells, mucus) (Fröhlich and Roblegg 2012). The absorption is estimated to be approximately 15- to 25-fold higher for nanoparticles (Desai et al. 1996). In line with these data, Jani et al. (1994) showed the distribution of orally administered TiO_2 particles in the liver, spleen, and lungs. Other studies have reported the presence of titanium in blood and tissues of mice after intravenous injection of nanoparticles (Sugibayashi et al. 2008). A similar observation was reported by van Ravenzwaay et al. (2009), who compared inhalation with an i.v. route of administration for two different TiO_2 particle sizes (20–30 nm or 200 nm) in male Wistar rats for up to 28 days.

Consequently, we studied the histomorphological alterations of these deposits in pulmonary tissues compared with the unexposed lung samples. An examination of unexposed adult lung samples revealed normal architecture of the alveolar sacs and alveoli. The lining pneumocytes contained euchromatic nuclei, numerous mitochondria, and regular lamellar inclusions. Additionally there were few interstitial cells with minimal interstitial spaces. However, after TiO_2 NP intake, there was thickening of the pulmonary interstitium, changes of the lamellar inclusion ultrastructure, pneumocytic apoptosis, and the presence of interstitial particle-laden macrophages. However, the infiltration of polymorph nuclear inflammatory cells was more pronounced after ingestion of TiO_2 NPs. Enhancement of these local effects was observed at the sites of particle retention. In addition, morphometric analysis showed significant thinning of the alveolar septa with no significant change in the MLI (an indication of the inter-alveolar wall distance) compared with the control group. From the observed results, it is suggested that nanoparticle-induced alveolar epithelial cell apoptosis might be the

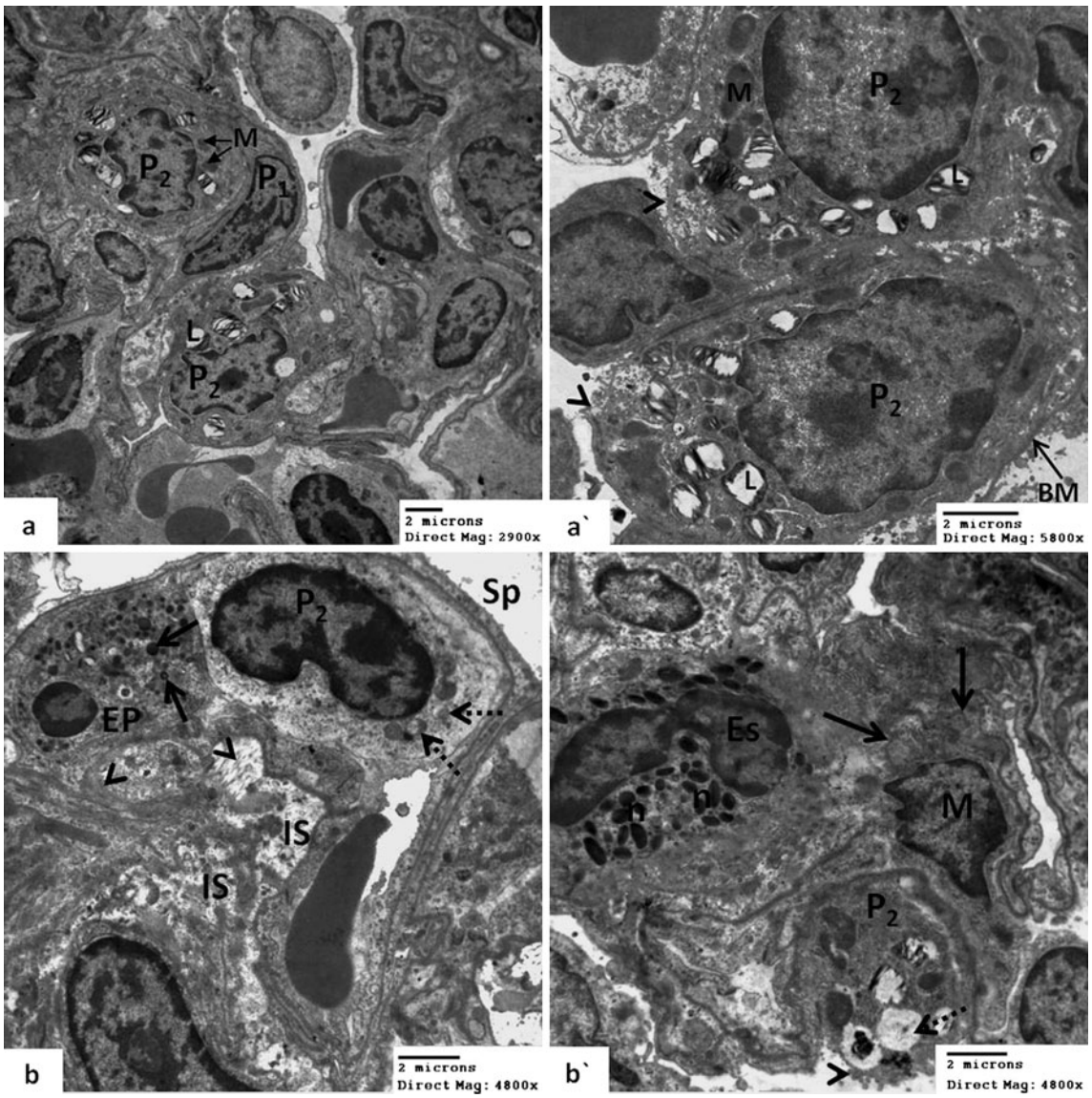

Fig. 4 Micrographs **a**, **a′** show the electron microscopic appearance of the control adult lung. The alveolar wall contains type II pneumocytes (P_2), recognizable by its lamellar inclusions (*L*) with an apparent pulmonary surfactant, and the cytoplasm is filled with numerous mitochondria (*M*). A type I pneumocyte (P_1) with an elongated euchromatic nucleus is also observed. The *right panel* shows type II pneumocytes resting on a basement membrane (*BM*), and a small proportion of its surface that is directly exposed to the alveolar space exhibits small microvilli (*arrowheads*) (uranyl acetate and lead citrate, Print Mag: **a** ×6,000—**b** ×12,000. Micrographs **b**, **b′** show the electron microscopic appearance of TiO_2 NP-treated adult lung with an apoptotic type II pneumocyte (P_2) with heterochromatic chromatin, atypical lamellar bodies (*dashed arrows*) and absent microvilli towards the alveolar space (*Sp*). The alveolar wall contains granulomatous epithelioid cell (*EP*), and its cytoplasm is burdened with electron opaque particles (*arrows*). There is an expansion in the interstitial spaces (*IS*) and dispersed collagen fibers (*arrowheads*). The *right panel* shows a type II pneumocyte (P_2) with an atypical empty lamellar body (*dashed arrows*) and short microvilli (*arrowhead*). An interstitial macrophage (*M*) is observed with an irregular nucleus and apical pseudopodia (*arrows*). An eosinophil (*Es*) is observed having the characteristic cytoplasmic stripped inclusions (*n*) (uranyl acetate and lead citrate, Print Mag: ×9,940)

cause of abnormal thinning of the alveolar septa and the abovementioned histological changes; namely, epithelial cell apoptosis, interstitial thickening, and abnormal surfactant that can induce partial diffusion block for gas exchange.

Similar histopathological changes were observed in the lungs after intratracheal instillation, intraperitoneal injection or oral instillation of TiO_2 particles to animals (Inoue et al. 2008; Liu et al. 2009). These findings of pulmonary inflammation are consistent with other studies showing that intratracheal exposure to nanoparticles (Chen et al. 2006) or inhalation (Borm and Kreyling 2004) can induce pulmonary inflammation. Additionally, pulmonary toxicity caused by TiO_2 NP inhalation has been reported (Afaq et al. 1998; Sun

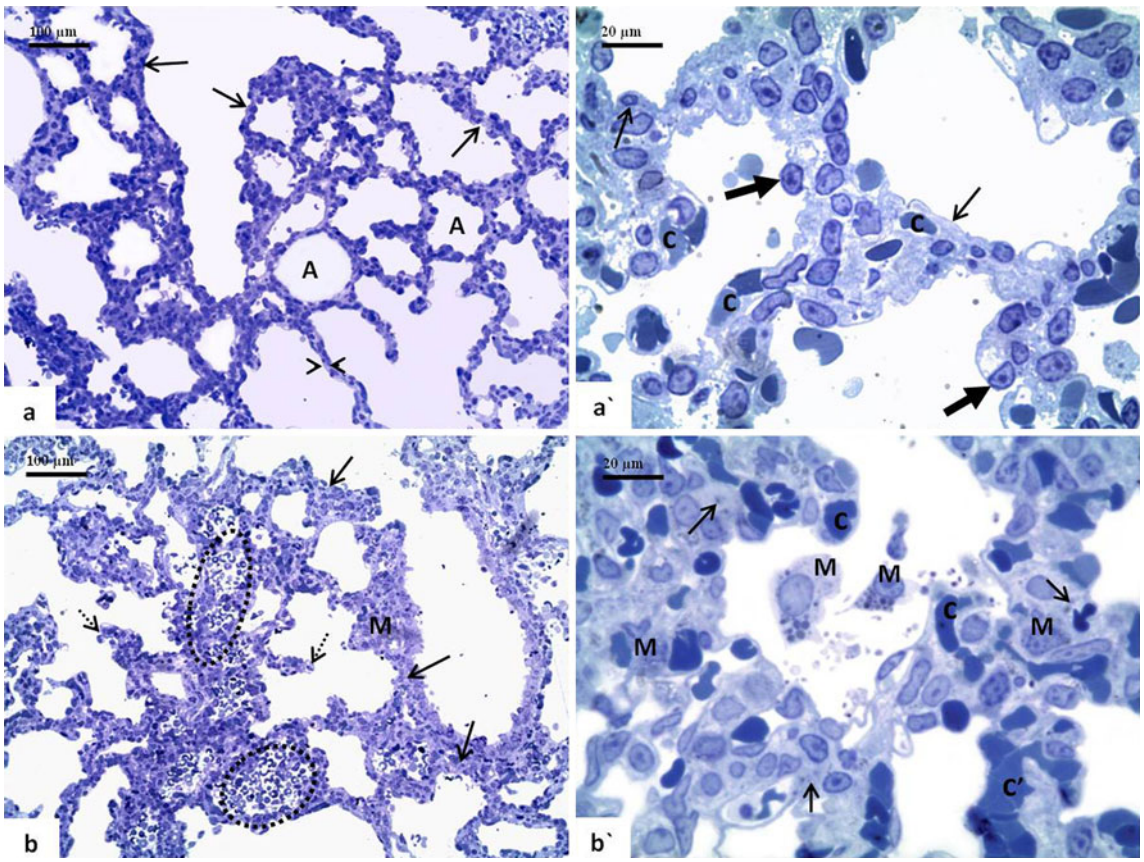

Fig. 5 Micrographs **a**, **a′** show the light microscopic appearance of neonatal lung from control mothers with smooth outlined channels and regularly shaped airspaces (*A*). The alveolar septa are uniform in width (*arrowheads*) and mostly completely formed. The *right panel* shows saccular walls lined with type I pneumocytes (*thin arrows*) and type II pneumocytes (*thick arrows*) that are surrounded by a plexus of blood capillaries (*c*). The alveolar septa are standardized in width and contain few interstitial cells. Micrographs **b**, **b′** show the light microscopic appearance of neonatal lung from TiO_2 NP-treated mothers. There are fewer airways with incomplete (*dashed arrows*) and clearly thickened septations (*arrows*). The alveolar septa show congested blood vessels (*circles*). The *right panel* shows apparent thickening of the primary septa with the presence of various interstitial cells and congested blood capillaries (*c′*). There are several macrophages present in the alveolar septa (*M*) and free within the airway spaces. Macrophages lie adjacent to septal capillaries, (*c*) and their cytoplasms are burdened with dense-stained particles (*arrows*) [**a**, **b** toluidine blue ×200—**a′**, **b′** toluidine blue ×1,000]

et al. 2004). Recent studies have shown that TiO_2 NPs produced only transient inflammatory effects that recovered after short-term exposure (Warheit et al. 2007). Even with subacute inhalation of these nanoparticles, the inflammatory response was sustained for only 2–3 weeks (Grassian et al. 2007). Our findings of inflammatory reaction and alveolar epithelial apoptosis are suggested to be involved in TiO_2 NP-induced pulmonary toxicity. Because TiO_2 NPs are widely used in cosmetics and food additives, these results may have important clinical implications regarding their safety (Weir et al. 2012).

In contrast, some authors have reported contradictory results regarding the measured MLI. Chen et al. (2006) found a slight increase in the MLI and in the airspace area on day 3 that significantly increased at the first week after administration of TiO_2 NPs and persisted until the second week. They concluded that TiO_2 NPs induced emphysema-like lung injury in mice. The discrepancy between our study and others is most likely attributed to differences in the treatment methods. Nevertheless, all studies did demonstrate that TiO_2 NPs at higher doses had serious toxicity to rat lungs.

Interestingly, Bermudez et al. (2004) found that there were significant inter-species differences in pulmonary response after exposure to TiO_2 particles. Their analysis of pulmonary parameters, including particle clearance from lungs, inflammation, proliferation of lung epithelial cells, and histopathologic alterations, showed that rats developed a more severe pulmonary inflammatory response than mice or hamsters.

In contrast, we studied the effects of maternal intake of TiO_2 NPs on the late-term neonatal lung. TEM sections displayed considerable black aggregates that were observed inside the alveolar epithelium, in the alveolar spaces and in the interstitium. These observations were confirmed by the analysis of data by EDX in conjunction

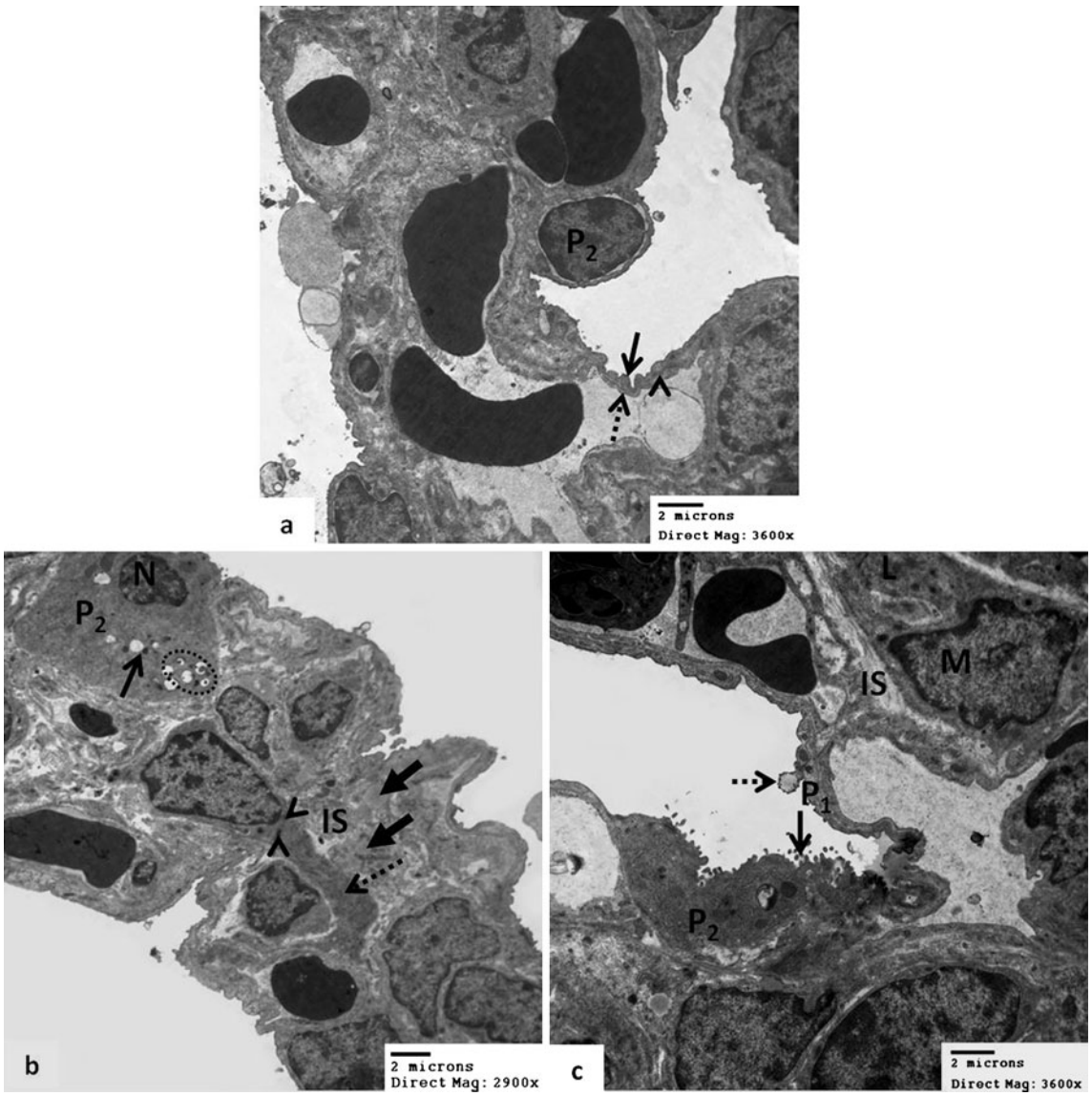

Fig. 6 Micrograph **a** shows the electron microscopic appearance of neonatal lung from control mother with a type II pneumocyte (P_2) inside a *circle* of the blood-air barrier formed as part of the peripheral cytoplasm of a type I pneumocyte (*arrow*) and that of the endothelium of the blood capillary (*dashed arrow*) that share a common basement membrane (*arrowhead*). Micrographs **b**, **c** show the electron microscopic appearance of neonatal lung from TiO_2 NP-treated mother with a primary septum with many interstitial cells. There is widening of the interstitial spaces (*IS*) with electron lucent vacuolated areas (*thick arrows*). A smaller type II pneumocyte (P_2) exhibits a shrunken dark and eccentric nucleus (*N*). The cytoplasm contains empty lamellar bodies (*arrows*); some lamellar bodies contain apparent atypical surfactant (*inside circle*). An interstitial macrophage (*M*) is observed with long pseudopodus (*dashed arrow*) and numerous lysosomes (*arrowheads*). The *right panel* shows widening of the interstitial spaces (*IS*) and a type I pneumocyte (P_1) with a pinocytotic vesicle (*dashed arrow*). Type II pneumocytes (P_2) appear with a dark apoptotic cytoplasm and few short microvilli (*arrows*). AN interstitial macrophage (*M*) is observed with an irregular nucleus and numerous lysosomes (*L*) (uranyl acetate and lead citrate, Print Mag: **a**, **c**, ×7,450; **b**, ×6,000)

with SEM. The detected TiO_2 NPs in the pulmonary tissue of neonatal pups suggests the transmission of these nanoparticles from mothers to their offspring, i.e., the ability of the TiO_2 nanoparticles to bypass the placental barrier. This is consistent with previous studies that demonstrated the embryotoxic role of a maternal intravenous injection of TiO_2 NPs or subcutaneous injections of anatase TiO_2 NPs (Takeda et al. 2009; Shimizu et al. 2009; Takahashi et al. 2010). After subcutaneous injection, TiO_2 accumulation was detected in the offspring cerebral cortex and olfactory bulb and numerous olfactory bulb cells and induced an altered expression of genes involved in brain development and cell death and a response to oxidative stress in the newborn pups (Shimizu et al. 2009).

Histomorphological examination of neonatal lungs at this age (21-day gestation) revealed the saccular stage of

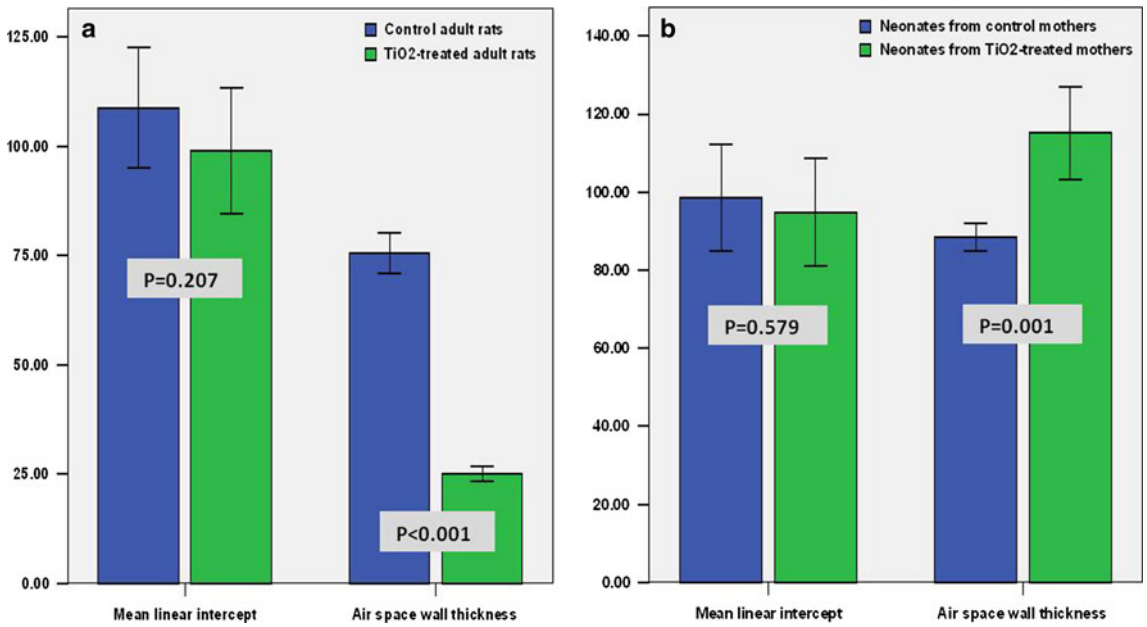

Fig. 7 *Bars* the morphometry of pulmonary acini in pregnant rats (**a**) and neonatal pups (**b**). Data are expressed as the mean ± SE. $*p < 0.05$ when the variables in the control and TiO_2 NP-treated groups are compared using Mann–Whitney test

development, which simulates lungs of preterm human babies at gestational ages between weeks 26 and 36 as documented in early studies (Burri 1991). Light and electron microscopic examination of neonates from control mothers revealed large thick-walled saccules with a smooth outline. Saccules were separated by thick primary interalveolar septa because of the presence of many layers of interstitial cells. This is associated with the observation of capillaries on both sides of the primary septa. Moreover, there were numerous type II pneumocytes with numerous lamellar inclusions and obvious microvilli. These observations were in accordance with previous studies (Adamson 1991).

Histological and morphometric analysis of neonatal lungs after maternal intake of TiO_2 NPs reveals variable shaped saccules with a significant increase in the thickness of the primary septa but with no significant change in the MLI compared with the control group. Moreover, there was focal thickening of the mesenchyme, poor septation, abnormal lamellar inclusions, pneumocytic apoptosis, and alveolar macrophage infiltration. TiO_2 NPs appeared to have been engulfed by interstitial and free alveolar macrophages. Nonetheless, the more pronounced observation was the infiltration of inflammatory cells. The increase in the septal thickness in pups versus its decrease in the mothers could be because of the presence of many interstitial cells in the primary interalveolar septa, which was confirmed by electron microscopic examination together with the focal deposition of the mesenchyme. However, in the mothers, the observed alveolar septal thinning could be a result of apoptotic changes and epithelial cell injury triggered by TiO_2 NP deposition in the pulmonary tissue.

It is suggested that the observed thickening of the mesenchyme between the airspaces together with the poor septation could lead to a partial diffusion block for gas exchange. Additionally, pneumocytic apoptosis of type II pneumocytes (producing pulmonary surfactants) and type I pneumocytes (lining the expanded alveoli) could affect alveolar maturation (Adamson 1991). The observed morphological alterations and pneumocytic apoptosis imply a morphological basis for respiratory failure in the neonatal rats. Ambalavanan et al. (2013) suggested that exposure of the developing lung to TiO_2 NPs may lead to ineffective clearance by macrophages and persistent inflammation with effects on lung development; this effect was confirmed in our study. This is consistent with Hussain et al. (2011) who observed that low, intrapulmonary doses of TiO_2 or gold NPs could aggravate pulmonary inflammation and airway hyperreactivity in a mouse model of diisocyanate-induced asthma. Furthermore, studies have also found that TiO_2 NPs cause genetic damage in mice (Trouiller et al. 2009).

In conclusion, the present results suggest the presence of TiO_2 NPs in maternal and neonatal pulmonary tissues after maternal oral intake of these particles, and indicate that the pulmonary response manifests as inflammatory lesions and saccular maldevelopment that may affect the risk of respiratory disorders in later life. Although additional studies are necessary to support these findings, they should be considered for a more accurate risk assessment of TiO_2

NP exposure, particularly during a complex biological status, such as pregnancy and the early stage of life.

Acknowledgments The authors gratefully acknowledge Deanship of Taibah University, Kingdom of Saudi Arabia for continuous help and support. We also thank the research assistances for their help in recording and filing the research data.

Conflict of interest The authors declare that there is no conflict of interest related to this study.

References

Adamson YVR (1991) Development of lung structure. In: Cristal RG, West JB et al (eds) The lung. Scientific Foundations Raven, New York, pp 663–670

Afaq F, Abidi P, Matin R, Rahman Q (1998) Cytotoxicity, pro-oxidant effects and antioxidant depletion in rat lung alveolar macrophages exposed to ultrafine titanium dioxide. J Appl Toxicol 18:307–312

Agarwal BK (1991) X-ray spectroscopy, 2nd edn. Springer, Berlin

Ambalavanan N, Stanishevsky A, Bulger A, Halloran B, Steele C, Vohra Y, Matalon S (2013) Titanium oxide nanoparticle instillation induces inflammation and inhibits lung development in mice. Am J Physiol Lung Cell Mol Physiol 304:152–161

Bermudez E, Mangum JB, Wong BA, Asgharian B, Hext PM, David B, Warheit DB, Everitt JI (2004) Pulmonary responses of mice, rats, and hamsters to subchronic inhalation of ultrafine titanium dioxide particles. Toxicol Sci 77:347–357

Borm PJ, Kreyling W (2004) Toxicological hazards of inhaled nanoparticles-potential implications for drug delivery. J Nanosci Nanotechnol 4:521–531

Braydich-Stolle LK, Schaeublin NM, Murdock RC, Jiang J, Biswas P, Schlager JJ, Hussain SM (2009) Crystal structure mediates mode of cell death in TiO2 nanotoxicity. J Nanopart Res 11:1361–1374

Burri PH (1991) Postnatal development and growth. In: Crystal RG, West JB, Weibel ER et al (eds) The lung. Scientific Foundations, Philadelphia, pp 1013–1026

Chen HW, Su SF, Chien CT, Lin WH, Yu SL, Chou CC, Chen JJ, Yang PC (2006) Titanium dioxide nanoparticles induce emphysema-like lung injury in mice. FASEB J 20:2393–2395

Chu M, Wu Q, Yang H, Yuan R, Hou S, Yang Y, Zou Y, Xu S, Xu K, Ji A, Sheng L (2010) Transfer of quantum dots from pregnant mice to pups across the placental barrier. Small 6:670–678

Desai MP, Labhasetwar V, Amidon GL, Levy RJ (1996) Gastrointestinal uptake of biodegradable microparticles: effect of particle size. Pharm Res 13:1838–1845

Fröhlich E, Roblegg E (2012) Models for oral uptake of nanoparticles in consumer products. Toxicology 27(291):10–17

Fujita K, Morimoto Y, Ogami A, Myojyo T, Tanaka I, Shimada M, Wang WN, Endoh S, Uchida K, Nakazato T, Yamamoto K, Fukui H, Horie M, Yoshida Y, Iwahashi H, Nakanishi J (2009) Gene expression profiles in rat lung after inhalation exposure to C60 fullerene particles. Toxicology 258:47–55

Glauert AM, Lewis PR (1998) Biological specimen preparation for transmission electron microscopy, 1st edn. Portland Press, London

Grassian VH, O'shaughnessy PT, Adamcakova-Dodd A, Pettibone JM, Thorne PS (2007) Inhalation exposure study of titanium dioxide nanoparticles with a primary particle size of 2 to 5 nm. Environ Health Perspect 115:397–402

Hougaard KS, Jackson P, Jensen KA, Sloth JJ, Löschner K, Larsen EH, Birkedal RK, Vibenholt A, Boisen AM, Wallin H, Vogel U (2010) Effects of prenatal exposure to surface-coated nanosized titanium dioxide (UV-Titan). A study in mice. Part Fibre Toxicol 7:16

Hussain S, Vanoirbeek JA, Luyts K, De Vooght V, Verbeken E, Thomassen LC, Martens JA, Dinsdale D, Boland S, Marano F, Nemery B, Hoet PH (2011) Lung exposure to nanoparticles modulates an asthmatic response in a mouse model. Eur Respir J 37:299–309

Inoue K, Takano H, Ohnuki M, Yanagisawa R, Sakurai M, Shimada A, Mizushima K, Yoshikawa T (2008) Size effects of nanomaterials on lung inflammation and coagulatory disturbance. Int J Immunopathol Pharmacol 21:197–206

Jani PU, McCarthy DE, Florence AT (1994) Titanium dioxide (rutile) particle uptake from the rat GI tract and translocation to systemic organs after oral administration. Int J Pharm 105:157–168

Jones CF, Grainger DW (2009) In vitro assessments of nanomaterial toxicity. Adv Drug Deliv Rev 61:438–456

Knudsen L, Weibel ER, Gundersen HJ, Weinstein FV, Ochs M (2010) Assessment of air space size characteristics by intercept (chord) measurement: an accurate and efficient stereological approach. J Appl Physiol 108:412–421

Koren G, Pastuszak A, Ito S (1998) Drugs in pregnancy. N Engl J Med 338:1128–1137

Li N, Nel AE (2011) Feasibility of biomarker studies for engineered nanoparticles: what can be learned from air pollution research. J Occupat Environ Med 53:74–79

Li B, Ze Y, Sun Q, Zhang T, Sang X, Cui Y, Wang X, Gui S, Tan D, Zhu M, Zhao X, Sheng L, Wang L, Hong F, Tang M (2013) Molecular mechanisms of nanosized titanium dioxide-induced pulmonary injury in mice. PLoS ONE 8:55563

Liang G, Pu Y, Yin L, Liu R, Ye B, Su Y, Li Y (2009) Influence of different sizes of titanium dioxide nanoparticles on hepatic and renal functions in rats with correlation to oxidative stress. J Toxicol Environ Health 72:740–745

Liu H, Ma L, Zhao J, Liu J, Yan J, Ruan J, Hong F (2009) Biochemical toxicity of nano-anatase TiO2 particles in mice. Biol Trace Elem Res 129(1–3):170–180

Oberdörster G, Oberdörster E, Oberdörster J (2005) Nanotoxicology: an emerging discipline evolving from studies of ultrafine particles. Environ Health Perspect 113:823–839

Saunders M (2009) Transplacental transport of nanomaterials. Wiley Interdiscip Rev Nanomed Nanobiotechnol 1(6):671–684

Scott VD, Love G (1994) Quantitative electron probe microanalysis, 2nd edn. Ellis Horwood, Chichester

Shimizu M, Tainaka H, Oba T, Mizuo K, Umezawa M, Takeda K (2009) Maternal exposure to nanoparticulate titanium dioxide during the prenatal period alters gene expression related to brain development in the mouse. Part Fibre Toxicol 6:article 20

Sugibayashi K, Todo H, Kimura E (2008) Safety evaluation of titanium dioxide nanoparticles by their absorption and elimination profiles. J Toxicol Sci 33(3):293–298

Sun D, Meng T, Loong TH, Hwa TJ (2004) Removal of natural organic matter from water using a nano-structured photocatalyst coupled with filtration membrane. Water Sci Technol 49:103–110

Takahashi Y, Shinkai Y, Mizuo K, Oshio S, Takeda K (2010) Prenatal exposure to titanium dioxide nanoparticles increases dopamine levels in the prefrontal cortex and neostriatum of mice. J Toxicol Sci 35(5):749–756

Takeda K, Suzuki KI, Ishihara A, Kubo-Irie M, Fujimoto R, Tabata M, Oshio S, Nihei Y, Ihara T, Sugamata M (2009) Nanoparticles transferred from pregnant mice to their offspring can damage the genital and cranial nerve systems. J Health Sci 55(1):95–102

Tian F, Razansky D, Estrada GG, Semmler-Behnke M, Beyerle A, Kreyling W, Ntziachristos V, Stoeger T (2009) Surface modification and size dependence in particle translocation during early embryonic development. Inhal Toxicol 21(1):92–96

Trouiller B, Reliene R, Westbrook A, Solaimani P, Schiestl RH (2009) Titanium dioxide nanoparticles induce DNA damage and genetic instability in vivo in mice. Cancer Res 69(22): 8784–8789

van Ravenzwaay B, Landsiedel R, Fabian E, Burkhardt S, Strauss V, Ma-Hock L (2009) Comparing fate and effects of three particles of different surface properties: nano-TiO2, pigmentary TiO2, and quartz. Toxicol Lett 186:152–159

Vlahovic G, Russell ML, Mercer RR, Crapo JD (1999) Cellular and connective tissue changes in alveolar septal walls in emphysema. Am J Respir Crit Care Med 160:2086–2092

Wang J, Zhou G, Chen C, Yu H, Wang T, Ma Y, Jia G, Gao Y, Li B, Sun J (2007) Acute toxicity and biodistribution of different sized titanium dioxide particles in mice after oral administration. Toxicol Lett 168:176–185

Warheit DB, Webb TR, Reed KL, Frerichs S, Sayes CM (2007) Pulmonary toxicity study in rats with three forms of ultrafine-TiO2 particles: differential responses related to surface properties. Toxicology 230(1):90–104

Weir A, Westerhoff P, Fabricius L, Hristovski K, von Goetz N (2012) Titanium dioxide nanoparticles in food and personal care products. Environ Sci Technol 46:2242–2250

Wigle DT, Arbuckle TE, Turner MC, Bérubé A, Yang Q, Liu S, Krewski D (2008) Epidemiologic evidence of relationships between reproductive and child health outcomes and environmental chemical contaminants. J Toxicol Environ Health B Crit Rev 11:373–517

Yokel RA, Macphail RC (2011) Engineered nanomaterials: exposures, hazards, and risk prevention. J Occup Med Toxicol 6:7

Zhang Q, Kusaka Y, Donaldson K (2000) Comparative injurious and proinflammatory effects of three ultrafine metals in macrophages from young and old rats. Inhal Toxicol 12:267–273

Zhang R, Niu Y, Li Y, Zhao C, Song B, Li Y, Zhou Y (2010) Acute toxicity study of the interaction between titanium dioxide nanoparticles and lead acetate in mice. Environ Toxicol Pharmacol 30(1):52–60